# Electron-impurity tunneling in selectively doped $n$-type $Al_xGa_{1-x}As/GaAs$ heterostructures

E. F. Schubert, A. Fischer, and K. Ploog
*Max-Planck-Institut für Festkörperforschung, Heisenbergstrasse 1, D-7000 Stuttgart 80, Federal Republic of Germany*
(Received 26 October 1984)

The interaction of the two-dimensional electron gas at the semiconductor interface of a selectively doped $n$-type $Al_xGa_{1-x}As/GaAs$ heterostructure grown by molecular-beam epitaxy with empty impurity levels in the $Al_xGa_{1-x}As$ layer is investigated both experimentally and theoretically. The electron subband energy levels in the triangular potential well of the heterostructure are calculated by a new method and are in excellent agreement with other approaches. The calculation of the electron-impurity tunneling process is based on a square-well potential shape to obtain solutions in an analytic and not in a numerical form. For experimental investigations we used time-resolved Hall effect and conductivity measurements combined with excitation by monochromatic illumination of the sample. The decay of the carrier concentration after illumination is monitored for more than 3 days at temperatures ranging from 20 to 150 K and is conclusively found to be nonexponential. Extrapolation of the decay to the dark concentration yields a total lifetime of photoconductivity of more than $10^{12}$ s at $T \leqq 77$ K. The optical threshold energies of $0.95 \leqq E_{do} \leqq 1.10$ eV for persistent photoconductivity coincides with the values for transient photoconductivity. This result demonstrates that both parts of the photoconductivity are caused by the same deep Si donor in the $Al_xGa_{1-x}As$ layer. The relative contributions to persistent photoconductivity of electron excitation from the deep Si donor in the $Al_xGa_{1-x}As$ layer as well as electron-hole generation in the GaAs layer are determined for a specific alloy composition of $Al_xGa_{1-x}As$. Electron-hole generation in the GaAs layer contributes only a minor part to the observed persistent photoconductivity of the heterostructure for alloy compositions $x \geqq 0.3$.

## I. INTRODUCTION

Modern electronic and photonic semiconductor devices are continuously scaled down to smaller sizes. The small dimensions provide new physical phenomena, including quantum effects of the two-dimensional electron gas[1,2] or ballistic transport effects.[3] In addition, tunneling phenomena are more important in structures of very small dimensions. Small-dimension semiconductor structures are generated by photolithography in the lateral direction and by epitaxy in direction normal to a semiconductor wafer. Among the various epitaxial methods, molecular-beam epitaxy (MBE) allows one to grow well-defined structures of semiconductors, doping profiles, and superlattices, and the technique has reached the ultimate physical limit of small dimensions by growing a GaAs/AlAs interface having the abruptness of one atomic monolayer.[4] Therefore, at present tunneling effects are more likely to occur normal to the surface than in the lateral direction, because miniaturization is much more advanced in the growth direction of epitaxial layers.

The dominant features of selectively doped (SD) $n$-type $Al_xGa_{1-x}As/GaAs$ heterostructures realized first with MBE (Ref. 5) are (i) a quasi-two-dimensional electron gas confined at the interface of the two semiconductors, (ii) a very high electron mobility at low temperatures where ionized impurity scattering dominates in bulk material, and (iii) sensitivity to light at low temperatures. Photoconductivity (PC) of selectively doped heterostructures is classified in transient photoconductivity [(TPC) (Ref. 6)] and persistent photoconductivity [(PPC) (Refs. 7 and 8)] for the decaying and the remaining part of the photoinduced carrier concentration, respectively.

In Figs. 1(a)—1(g) we have illustrated the most important tunneling mechanisms in semiconductor structures.[9]

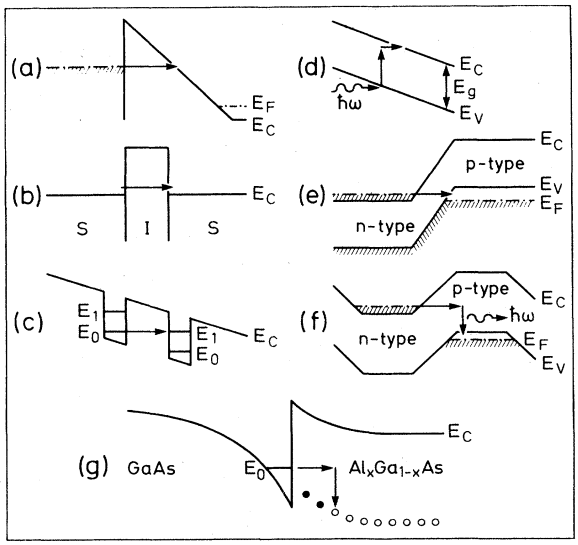


FIG. 1. (a)—(c) Intraband and (d)—(f) interband tunneling mechanisms in semiconductor structures; (a) Fowler-Nordheim tunneling, (b) semiconductor-insulator-semiconductor tunneling, (c) resonant tunneling, (d) Franz-Keldysh tunneling, (e) $p$-$n$ junction tunneling, and (f) tunneling in doping superlattices. (g) Electron-impurity tunneling occurs in selectively doped $Al_xGa_{1-x}As/GaAs$ heterostructures.

 

In *intraband tunneling* the electrons (holes) remain in the conduction (valence) band before and after tunneling. This feature is provided by Fowler-Nordheim tunneling[10] [Fig. 1(a)], semiconductor-insulator-semiconductor (*S-I-S*) tunneling[11] [Fig. 1(b)], and resonant tunneling between subbands of two quantum wells[12] [Fig. 1(c)]. During *interband tunneling* electrons tunnel from the conduction band to the valence band or vice versa. This feature is observed in the Franz-Keldysh effect [Fig. 1(d)], in *p-n* junctions of Esaki diodes [Fig. 1(e)], and during radiative recombination in doping superlattices [Fig. 1(f)].[13] The electron impurity tunneling of Fig. 1(g) occurs in selectively doped (SD) heterostructures. In this tunneling mechanism electrons of the two-dimensional electron gas (2D EG) at the semiconductor interface penetrate the barrier provided by $Al_xGa_{1-x}As$ via tunneling and subsequently recombine with an impurity level localized in the forbidden gap of the barrier material. Consequently, the 2D EG concentration decreases during electron-impurity tunneling so that a low-temperature transient photoconductivity (TPC) effect is observed in SD heterostructures after illumination.[6]

In this paper we investigate in detail the electron impurity tunneling in selectively doped *n*-type $Al_xGa_{1-x}As/GaAs$ heterostructures, and we analyze the experimental data quantitatively. The penetration of the electron wave function into a square-well potential is obtained as an analytic function using the Wentzel-Kramers-Brillouin (WKB) method. The recombination probability is calculated via the overlap integral of the 2D EG and the impurity wave function. During experiments the electron excitation is achieved by illuminating the sample with monochromatic light of wavelengths ranging from 1700 to 800 nm. The threshold wavelength of both the persistent and transient photoconductivity is thus obtained and compared. In addition, the contribution of band-to-band electron-hole generation in the GaAs layer to persistent photoconductivity is estimated quantitatively. Finally, the decay of the free-electron concentration is analyzed for a time period of more than 72 h at low temperatures after the illumination has been switched off. This analysis clearly reveals the nonexponential decay of photoexcited carrier concentration with time.

The paper is organized as follows. In Sec. II A the energy of the lowest subband of a triangular potential well is calculated by a simple method. The decay of the 2D EG carrier concentration due to electron-impurity tunneling is calculated in Sec. II B. After the description of some important experimental details in Sec. III we show the distinct nonexponential decay of the carrier concentration with time in Sec. IV A. In Sec. IV B the long-term decay of the carrier concentration is measured and discussed. In Sec. IV C we determine the optical threshold wavelength for the persistent and transient part of photoconductivity. A conclusion is given in Sec. V.

## II. THEORY

### A. Subband energies in a finite and infinite triangular potential well

We first show that the energy of the bottom of the lowest electron subband at the heterostructure interface is obtained with good accuracy by a simple calculation. In our approach we match the electron—de Broglie wavelength to the width of the potential well. The shape of the potential well at the semiconductor interface of a selectively doped *n*-type $Al_xGa_{1-x}As/GaAs$ heterostructure is usually taken to be triangular. Electrons are confined within the two barriers of the quantum well. *At the $Al_xGa_{1-x}As$ side* of the quantum well the conduction-band edge changes abruptly with the spatial coordinate $z$ due to the conduction-band discontinuity of the two semiconductor materials.[14] *At the GaAs side* of the quantum well the conduction-band edge $E_C$ changes continuously with the spatial coordinate $z$ and is given by the amount of charge $qN_D^{2D}$ transferred from the doped *n*-type $Al_xGa_{1-x}As$ to the GaAs according to

$$dE_C/dz = q\mathscr{E} = q^2N_D^{2D}/\epsilon\ , \tag{1}$$

where $q$ is the elementary charge and $\epsilon$ is the permittivity of GaAs. The charge $qN_D^{2D}$ transferred from the doped *n*-type $Al_xGa_{1-x}As$ to the GaAs is assumed to be equal to the charge of the two-dimensional electron gas $qn_{2D\ EG}$. The electron—de Broglie wavelength is now fitted into the triangular potential well, depicted in Fig. 2, such that the wave function does not penetrate the barriers. The electron—de Broglie wavelength $\lambda_{dB}$ is given by

$$\lambda_{dB} = h/(2Em^*)^{1/2} \tag{2}$$

and matches into the quantum well according to

$$\tfrac{1}{2}(i+1)\lambda_{dB}(E_i) = z_i(E_i) \quad \text{for } i = 0,1,2,\ldots, \tag{3}$$

where $z_i(E_i)$ is the spatial width of the well at energy $E_i$ given by Eq. (1). In this way the energies of the subbands in the potential well are obtained

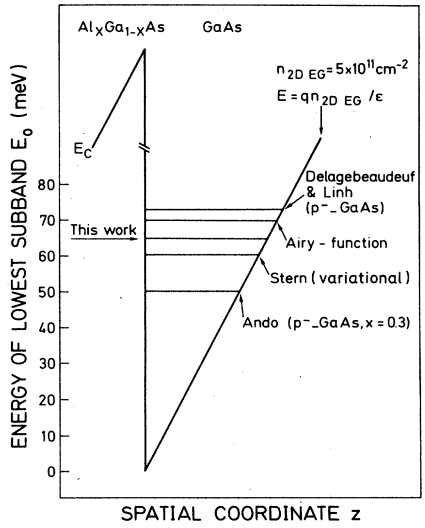


FIG. 2. Energies of the bottom of the lowest subband in a triangular potential well at the $GaAs/Al_xGa_{1-x}As$ interface. In our present work the subband energy is obtained by matching the electron—de Broglie wavelength to the potential well width. Other approaches include self-consistent calculations by Ando (Ref. 16), variational calculations by Stern (Ref. 15), by the Airy function, and values based on experimental data by Delagebeaudeuf and Linh (Ref. 18).

$$E_i=\tfrac{1}{2}(i+1)^{2/3}\left[\frac{q^2hn_{2D\,EG}}{\epsilon(m^*)^{1/2}}\right]^{2/3} \quad \text{for } i=0,1,2,\ldots . \tag{4}$$

This simple result gives a first general trend of the subband energies depending on familiar parameters and on the electron concentration of the triangular well. The amplitude of the wave function is taken to be zero at the two barriers, i.e., tunneling effects are neglected. Furthermore, band bending due to free carriers is not taken into account and the potential well has a strict triangular shape as illustrated in Fig. 2. Consequently the calculation presented here is not self-consistent.

Quantitatively the energy of the lowest subband $E_0$ obtained by the method proposed here is in good agreement with the results obtained by other approaches. A comparison of lowest subband energies obtained by several authors is shown in Fig. 2 for an interface carrier concentration of $n_{2D\,EG}=5\times10^{11}$ cm$^{-2}$. Stern[15] calculated the lowest subband energy by a variational method which neglects the penetration of the wave function only at the $Al_xGa_{1-x}As$ side. Ando[16] used a numerical self-consistent method and obtained a comparatively low subband energy. The Airy function yields the exact solution of the infinite triangular-well problem. Approximate values for the lowest subband energy obtained by the Airy function have been reviewed by Ando *et al.*[17] Delagebeaudeuf and Linh[18] obtained the energy of the lowest subband by assuming the dependence of $E_0=\gamma n_{2D\,EG}^{2/3}$ and by adjusting the parameter $\gamma$ for the best agreement with experimental results. When we consider the scattering of the various subband energies obtained by different methods and depicted in Fig. 2, our approach based on the particle-wave character of the electron is a good trade-off between accuracy and simplicity of the calculation.

### B. Electron-impurity tunneling

The principle of the electron-impurity tunneling at a heterointerface is depicted in Fig. 3. Electrons are excited optically (1) from an impurity level and relax into the square-shaped potential well. In this situation, however, the system is in a metastable state, since there are empty states at lower energy available. Consequently electrons can recombine (are trapped) by means of a tunneling process (2) with the impurity level (3). The recombination of the electrons with the impurities results in a transient photoconductivity [(TPC) (Ref. 6)], i.e., a decay of the free carrier concentration with time. We will calculate the decay of the carrier concentration *analytically* using the square-well potential depicted in Fig. 3. Band bending effects due to ionized impurities and by free electrons are not taken into account.

At the semiconductor heterointerface a conduction-band discontinuity $\Delta E_C$ of

$$\Delta E_C=\alpha\,\Delta E_g \tag{5}$$

occurs where $\Delta E_C$ is the difference of the conduction-band energies of the two materials. Dingle[14] estimated the parameter $\alpha$ to be 0.85; however, smaller estimations have also been proposed.[19] In the potential well electrons popu-

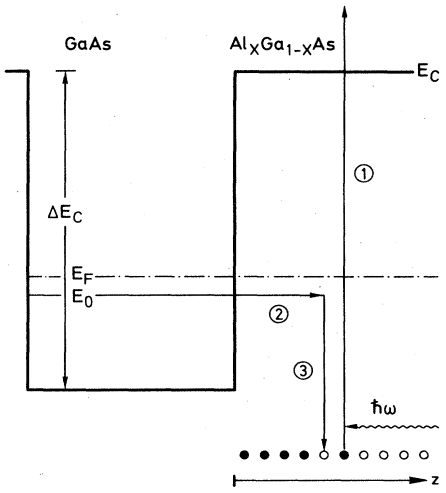


FIG. 3. Principle of electron-impurity tunneling at a semiconductor interface. Electrons are lifted by optical excitation into the conduction band (1) and relax into the potential well. Then electrons take part in a tunneling (2) assisted recombination (3) and reach thermal equilibrium.

late quantized energy levels due to size quantization. We assume that only the lowest subband of energy $E_0$ is occupied. The wave function of the 2D EG, $\Psi_{2D\,EG}(z)$, amounts to $\Psi_{2D\,EG}(0)=\Psi_I$ at the interface and decays in the $Al_xGa_{1-x}As$ barrier according to

$$\begin{aligned}\Psi_{2D\,EG}&=\Psi_I\exp\{-[2m^*(\Delta E_C-E_0)]^{1/2}z/\hbar\}\\&=\Psi_I\exp(-z/z_0)\,,\end{aligned} \tag{6}$$

where $z$ is the spatial coordinate depicted in Fig. 3, $m^*$ is the effective electron mass, and $\hbar$ is Planck's constant divided by $2\pi$. The recombination probability of the electron with the impurity is obtained via the overlap integral of the electron and the impurity wave function. The lifetime $\tau(z)$ of an empty impurity level in the $Al_xGa_{1-x}As$ therefore increases with its distance from the interface $z$ due to the exponential decay of the electron wave function given by

$$\tau(z)=\tau_0\exp(z/z_0)\,. \tag{7}$$

The lifetime $\tau_0$ is the mean lifetime of an empty impurity level localized exactly at the semiconductor interface.

The time-dependent carrier concentration of the two-dimensional electron gas, $n_{2D\,EG}(t)$, and its difference to the concentration under illumination, $\Delta n_{2D\,EG}(t)$, are

$$\begin{aligned}\Delta n_{2D\,EG}(t)&=n_{2D\,EG}^{ill}-n_{2D\,EG}(t)\\&=N_{TPC}\int_0^\infty\{1-\exp[-t/\tau(z)]\}dz\,.\end{aligned} \tag{8}$$

$N_{TPC}$ is the impurity concentration in the $Al_xGa_{1-x}As$ layer depicted in Fig. 3. The substitution of $u=\exp(-z/z_0)$ yields

$$\Delta n_{2D\,EG}(t)=-z_0N_{TPC}\int_1^0[1-\exp(-t^*u)](1/u)du\,. \tag{9}$$

The normalized time $t^*$ is given by $t^*=t/\tau_0$. The expan-

sion of the integrand to a power series (Taylor series),

$$\Delta n_{2D\,EG}(t)=z_0 N_{TPC}\int_1^0\left[-\frac{t^*}{1!}+\frac{(t^*)^2u}{2!}-\frac{(t^*)^3u^2}{3!}+\cdots\right]du\ , \tag{10}$$

followed by integration yields

$$\Delta n_{2D\,EG}=z_0 N_{TPC}\left[\frac{t^*}{1\times 1!}-\frac{(t^*)^2}{2\times 2!}+\frac{(t^*)^3}{3\times 3!}-\cdots\right]. \tag{11}$$

The decrease of the carrier concentration in the 2D potential well due to electron-impurity tunneling is expressed analytically in Eq. (11) by using a power series. The result is illustrated in Fig. 4 (bottom curve). There are two more power series which appear similar to that of Eq. (9). In particular, the exponential function

$$1-\exp(-t^*)=\frac{t^*}{1!}-\frac{(t^*)^2}{2!}+\frac{(t^*)^3}{3!}-\cdots \tag{12}$$

and the logarithmic function

$$\ln(1+t^*)=\frac{t^*}{1}-\frac{(t^*)^2}{2}+\frac{(t^*)^3}{3}-\cdots \tag{13}$$

are related to the exact solution. In these two power series only the denominator is changed as compared to Eq. (11).

For long times $t^*$ the *exponential* function saturates, and the saturated value is equal to one. This means that electrons recombine only with impurity levels within the distance $z_0$ from the interface. Consequently the 2D carrier concentration that relaxes is $N_{TPC}z_0$. In contrast, the *logarithmic* function of Eq. (13) does not saturate even for long times $t$. In Fig. 4 the three functions are depicted for comparison. The figure clearly reveals that the exact solution according to Eq. (11) decays most strongly. The logarithmic function is similar to the exact solution. For very short times, all the three functions shown in Fig. 4 decay in a similar manner. For long times, however, only the logarithmic and the exact solution are comparable. In addition the curves of Fig. 4 demonstrate that the decay of the carrier concentration is clearly nonexponential. While the exponential function saturates for long times, the exact solution does not saturate.

An approximate result for the decay of the carrier concentration is obtained in the following way. Equation (9) is differentiated with respect to $t^*$, and furthermore the normalized time $t^*$ is assumed to be much larger than 1, so that one obtains

$$\frac{d}{dt^*}\Delta n_{2D\,EG}(t^*)=z_0 N_{TPC}\int_1^0-\exp(-t^*u)du$$

$$\simeq z_0 N_{TPC}(1/t^*)\ . \tag{14}$$

This dependence of the current per unit area on the time according to $j(t)\sim t^{-n}$ $(0<n\leqq 1)$ is known as the *Curie–von Schweidler law* and has its origin at the beginning of the century.[20] The following integration yields

$$\Delta n_{2D\,EG}(t^*)\simeq z_0 N_{TPC}(\ln t^*+C)\ , \tag{15}$$

where $C$ is an integration constant. The logarithmic time dependence is, however, an *approximate* solution, and is less accurate to the exact solution of Eq. (11). Recently the logarithmic time dependence of the carrier concentration was found independently by Queisser[21] and some GaAs samples seemed to obey this dependence.

The speed of the carrier decay slows down for long

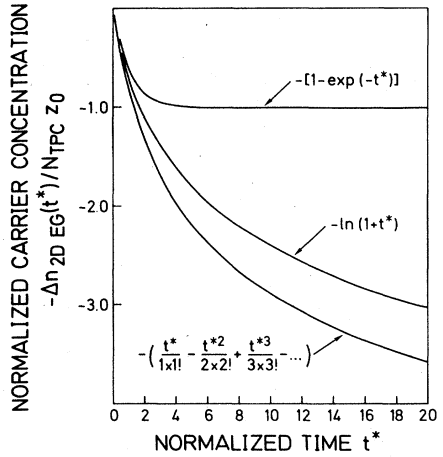


FIG. 4. Theoretical decay of the carrier concentration during electron-impurity tunneling. The bottom curve represents the exact solution obtained by the WKB method. The curve in the middle given by the logarithmic function (Curie–von Schweidler law) is a good approximation for the exact solution. The top curve indicating exponential decay deviates significantly from the exact solution. Therefore, electron-impurity tunneling yields a clear nonexponential decay of the electron concentration.

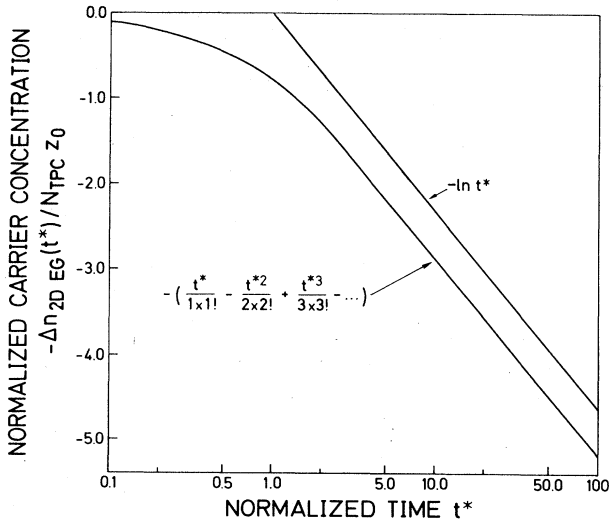


FIG. 5. Normalized calculated decay of the carrier concentration on a logarithmic time scale. The carrier concentration decreases linearly on the logarithmic time scale for $t^*\geqq 1$, that is $t\geqq\tau_0$, where $\tau_0$ is the mean lifetime of an empty impurity level at the interface.

times after switching off the exciting illumination. To investigate the long-term decay the carrier concentration is conveniently plotted on a logarithmic time scale. In Fig. 5 we show the theoretical solution of the decay caused by electron-impurity tunneling in a logarithmic time scale. For normalized times $t^* \leq 1$ ($t \leq \tau_0$), the function decays only negligibly. For normalized times $t^* \geq 1$ ($t \geq \tau_0$), the function decreases linearly on the logarithmic time scale. This behavior is characteristic to both the exact solution of Eq. (11) and the logarithmic function of Eqs. (13) and (15) which is included in the plot of Fig. 5. In this range the logarithmic decay is thus a good approximation to the exact solution.

## III. EXPERIMENTAL

The selectively Si-doped $n$-type $Al_xGa_{1-x}As/GaAs$ heterostructures were grown in a molecular-beam epitaxy (MBE) system of the quasihorizontal evaporation type which comprises a continuously azimutally rotating substrate holder and a liquid-$N_2$ cryoshroud encircling the entire growth region. The heterostructures were deposited on (100)-oriented semi-insulating GaAs substrates at a growth temperature of 650 °C. Since Al and Ga have very similar atomic radii of 1.41 and 1.43 Å, respectively, the two semiconductors AlAs and GaAs have comparable lattice constants of 5.6605 and 5.6533 Å, respectively. Therefore no special attention is required to the lattice match at the interface of the heterostructure. The layer sequence of the SD heterostructures includes an undoped 1-$\mu$m-thick GaAs buffer layer with a residual doping concentration below $10^{15}$ cm$^{-3}$, an undoped $Al_xGa_{1-x}As$ spacer layer of thickness 10 nm, a Si-doped $n$-type $Al_xGa_{1-x}As$ layer of thickness 50 nm, and an undoped GaAs cap layer with a thickness of 10—20 nm. Details of the growth procedure have been described elsewhere.[22]

The Hall-effect and resistance measurements were performed on mesa-etched Hall bars having six potential probes and two current contacts. The samples were mounted in a continuous flow He cryostat and the measurements are controlled by a computer. The time-dependent carrier concentration and the conductivity were determined by monitoring the Hall voltage and the voltage along the Hall bar, respectively, after the exciting illumination has been switched off. Special care was taken for a high reproducibility of the measurements. For monochromatic illumination we used a high-temperature tungsten iodine lamp with the light passing a grating monochromator with 675 grooves per 1 mm (Bausch and Lomb). Optical filters with cutoff wavelength at 780 and 1000 nm were used in addition to the monochromator. Furthermore, we employed a 2-mm-thick Si filter, having a cutoff wavelength of about 1100 nm.

## IV. RESULTS AND DISCUSSION

### A. Nonexponential decay of carrier concentration

When a selectively doped $n$-type $Al_xGa_{1-x}As/GaAs$ heterostructure is cooled down from room temperature in the dark, the carrier concentration decreases and reaches a saturated value at a temperature of 100 K. Below this temperature, the carrier concentration remains constant down to 4.2 K.[23,24] The freeze out of carriers in SD heterostructures is not a heterojunction-induced phenomenon but a bulk property of $n$-type $Al_xGa_{1-x}As$. We have recently shown[24] that this material exhibits two types of donors of different thermal ionization energy. Both donors are related to the Si impurity. One type of donor is shallow hydrogen-atom-like and follows the effective-mass theory. The other donor has a rather large thermal ionization energy of $140 \pm 10$ meV and does not follow the effective-mass model. The two types of donors were therefore labeled the shallow and deep donor of Si-doped $n$-type $Al_xGa_{1-x}As$.[24] The deep donor freezes out at low temperatures and is therefore the origin of the decrease of the carrier concentration at low temperatures in both bulk-type $n$-type $Al_xGa_{1-x}As$ and in SD $n$-type $Al_xGa_{1-x}As/GaAs$ heterostructures.

When a selectively doped heterostructure is exposed to light of energy below the band gap of both GaAs and $Al_xGa_{1-x}As$ at low temperatures the carrier concentration increases. Electrons are excited from the deep Si donor in $Al_xGa_{1-x}As$. After the illumination has been turned off, the carrier concentration decreases again, but this decrease slows down strongly after a few minutes. On a linear time scale the decay of the carrier concentration is rather fast for short times but then it slows down and apparently ceases. Therefore, the decaying and the remaining parts of the photoconductivity (PC) are referred as the transient part of photoconductivity (TPC) and the persistent part of photoconductivity (PPC), respectively. The transient part decays during the first few minutes after termination of the exciting illumination. The persistent part is the remaining photoconductivity which is observed after some minutes on a linear time scale for a long time. The saturated carrier concentration is therefore referred to as $n^{\infty}_{2D\,EG}$.

The decay of the carrier concentration is expressed in terms of a time constant $\tau(t)$ which itself depends on time, i.e.,

$$n_{2D\,EG}(t) - n^{\infty}_{2D\,EG} = \Delta n_{2D\,EG} \exp[-t/\tau(t)] \, . \tag{16}$$

Here $\Delta n_{2D\,EG}$ is the amplitude of the total decay of the carrier concentration. The time constant $\tau(t)$ increases with time so that the decay slows down. The physical background of an increasing time constant is that the electrons recombine with impurity levels located further away from the interface. In Fig. 6 the observed 2D minus the saturated carrier concentration is plotted on a logarithmic scale versus time. The plot clearly shows that the speed of the decay slows down. If the decay would be purely exponential, the slope of the curve should be constant. However, the observed slope of the curve changes drastically, i.e., the decay is definitely nonexponential. Consequently electron-impurity tunneling at a heterointerface is a phenomenon which yields a nonexponential decay law. The time constant $\tau$ is defined as the inverse slope of the curve depicted in Fig. 6:

$$\tau^{-1} = d[\ln(n_{2D\,EG}(t) - n^{\infty}_{2D\,EG})]/dt \, . \tag{17}$$

The time constant $\tau_0$ which applies after turning off the

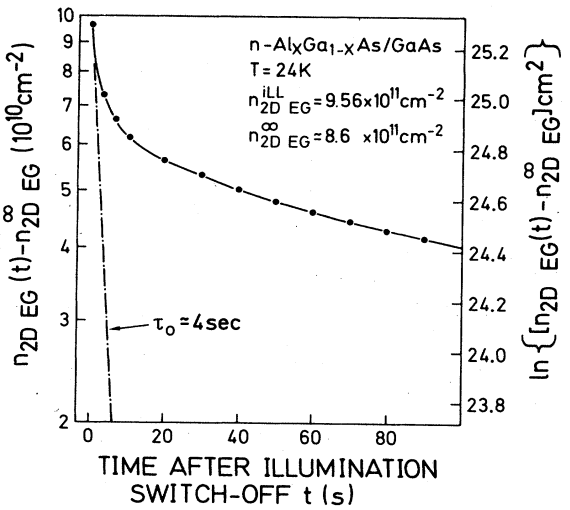


FIG. 6. Decay of the carrier concentration versus time observed in a selectively doped heterostructure. A nonexponential decay of the carrier concentration is evident, because the experimental points are *not* on a straight line. The time $\tau_0$ which applies to the initial decay is determined to be $\tau_0=4$ s.

exciting illumination is now easily obtained from Fig. 6 and is evaluated to be $\tau_0=4$ s. This time constant, however, is only valid for very small times after terminating the illumination. We have measured the decay not only for several minutes but for several days. In Fig. 7 the observed decay of the carrier concentration is shown on a much longer timescale comprising three days. In a similar manner as in Fig. 6, the time constant increases continuously throughout the three days. Since the measurement has to be performed at low temperatures, the measuring time is only limited by the amount of liquid He available in the container.

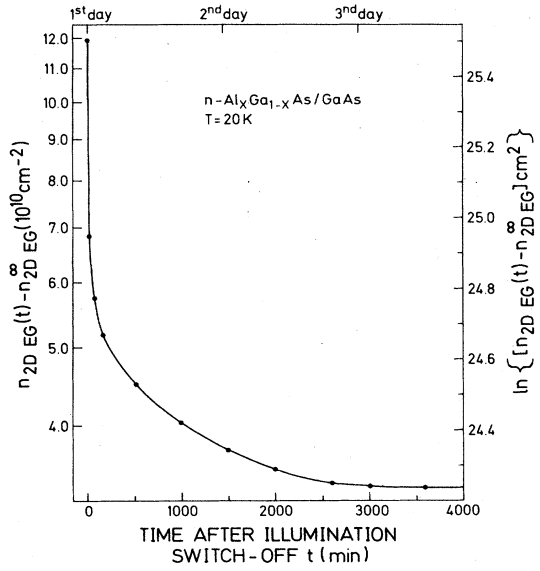


FIG. 7. Decay of the carrier concentration versus time of a selectively doped heterostructure on a longer timescale. Again the nonexponential decay of the carrier concentration is evident, because the experimental points do not form a straight line. The continuous change of the slope of the curve indicates a continuously increasing time constant $\tau$, because the recombination takes place with impurity levels located further away from the interface.

### B. Decay of carrier concentration on a logarithmic timescale

In Sec. II we have shown that the decay of the two-dimensional carrier concentration after terminating the illumination should be very similar to the logarithmic function of Eqs. (13) and (15) and that the carrier concentration should decay linearly on a logarithmic time scale. We measured the time-dependent carrier concentration for three days after terminating the illumination, and we performed measurements at four different sample temperatures. The results plotted on a logarithmic timescale are shown for the different temperatures in Figs. 8–10. At low temperature (Fig. 8) the carrier concentration decreases slowly for small times in this logarithmic time plot, as predicted by theory (see also the theoretical decay plotted in Fig. 5). For times between $10^2$ and $10^3$ s the curve behaves linearly. Now the time $t$ is larger than $\tau_0$ so that the concentration is expressed in terms of a simple logarithmic function [see also Eq. (15)]

$$\Delta n_{2D\,EG}(t)=N_{TPC}z_0[\ln(t/\tau_0)+C]\ . \tag{18}$$

Rearrangement and differentiation of the equation yields

$$\tau_0^{-1}=\frac{d}{dt}\exp\left[\frac{\Delta n_{2D\,EG}(t)}{N_{TPC}z_0}\right]\ . \tag{19}$$

It is thus possible to evaluate $\tau_0$ by a second independent method from the plot of Fig. 8 if the parameters $N_{TPC}$ and $z_0$ are known. These parameters are estimated to be $z_0\simeq 0.7$ nm according to Eq. (6) and $N_{TPC}$

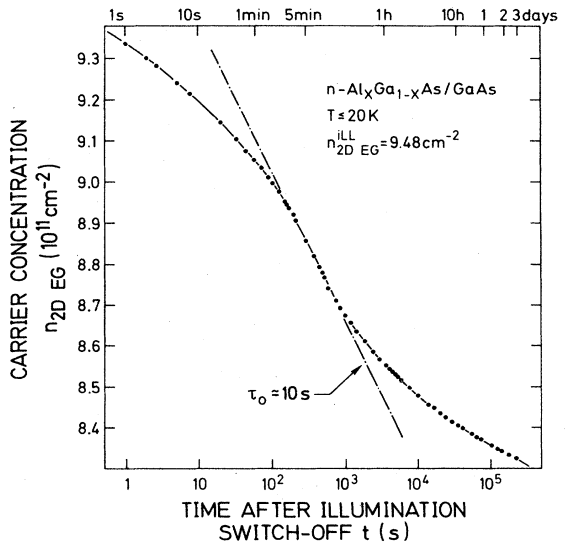


FIG. 8. Two-dimensional carrier concentration measured at $T=20$ K after the illumination is terminated. The time constant $\tau_0$ determined from the linear part of the decay is $\tau_0=10$ s.

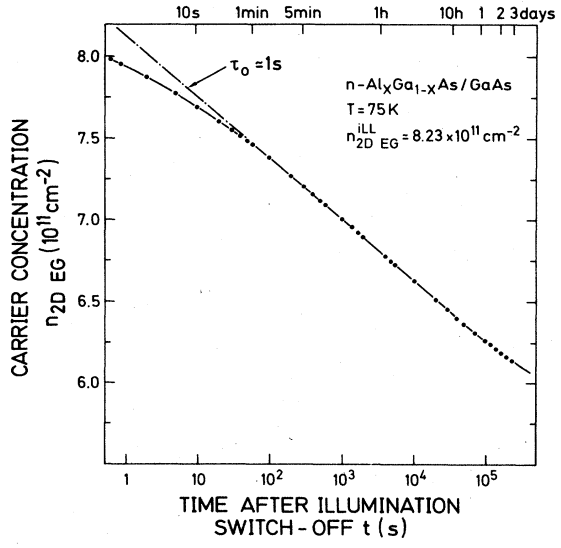


FIG. 9. Two-dimensional carrier concentration measured at $T=75$ K after the illumination is terminated. The time constant $\tau_0$ determined from the linear part of the decay is $\tau_0=1$ s. The extrapolation of the carrier concentration to its dark value yields a time of more than $10^{12}$ s ($\simeq 3\times 10^4$ years).

$\simeq 1\times 10^{17}$ cm$^{-3}$.[6] In this way we obtain the time constant of $\tau_0\simeq 10$ s as indicated in Fig. 8. The time constant determined from Figs. 6 and 8 should be equal since the samples and the measuring temperature are the same. The values are indeed roughly comparable and deviate by a factor of 2.5.

In Fig. 9 we show the carrier concentration versus logarithmic time measured at a temperature of 75 K after switching off the exciting illumination. The plot reveals an excellent linear dependence of the carrier concentration on time from 1 to more than $10^5$ s, i.e., during nearly 6 orders of magnitude. The time constant of the initial decay $\tau_0$ determined according to the described procedure yields a value of $\tau_0\simeq 1$ s. This value is about 10 times shorter than the time constant at 20 K. However, tunneling phenomena are known to be independent of temperature. The smaller time constant at higher temperature is therefore due to a change of the capture cross section of the involved impurity. Zhou *et al.*[25] have shown that the capture cross section of the deep Si donor in $n$-type $Al_xGa_{1-x}As$ indeed increase with temperature.

The dashed-dotted straight line depicted in Fig. 9 is now extrapolated to the initial carrier concentration in the dark $n_{2D\ EG}^{dark}\simeq 3\times 10^{11}$ cm$^{-2}$. This extrapolation determines the time, at which all photoexcited carriers have recombined with their parent impurities and are again in thermal equilibrium. As a result we find that the carrier concentration in the dark is reached after a time longer than $10^{12}$ s, i.e., more than $3\times 10^4$ years at $T\leqq 20$ K which represents an extremely long time.

At temperature above 100 K the decay of photoconductivity is even stronger. In Fig. 10 the carrier concentration is plotted versus time after illumination for the two temperatures of 125 and 150 K. At 150 K the carrier concentration saturates after approximately $10^3$ s and does not significantly change after this time. At saturation the selectively doped heterostructure has reached thermal equilibrium conditions. All photoexcited carriers have recombined with their parent impurities. The carrier concentration of $2.75\times 10^{11}$ cm$^{-2}$ corresponds to the electron concentration in the dark obtained by the Hall-effect measurement.

Comparison of the electron concentrations reached during illumination $n_{2D\ EG}^{ill}$ and depicted in Figs. 8–10 reveals a decrease at high temperatures. This decrease of carrier concentration is due to the larger recombination rate of electrons and the impurity at higher temperatures. The generation rate, however, remains constant since the illumination is not changed with temperature.

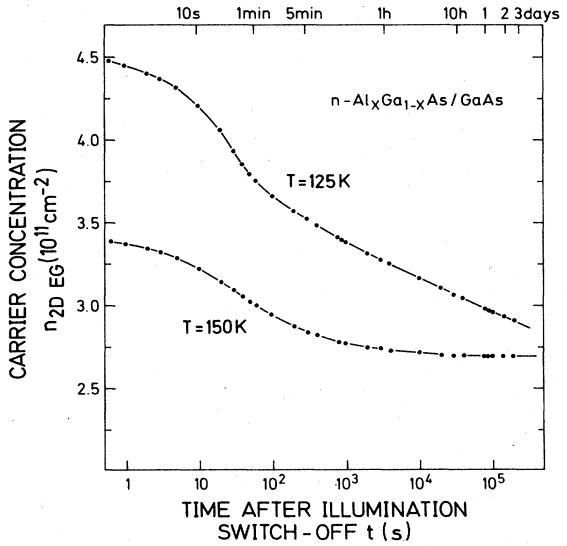


FIG. 10. Two-dimensional carrier concentration measured at $T=125$ and 150 K after the illumination is terminated. The saturation at $T=150$ K after $10^3$ s is due to a complete recombination of all photoexcited electrons with their parent impurities.

### C. Optical threshold of photoconductivity

Photoconductivity in semiconductors may have different physical origins. It is therefore convenient to classify photoconductivity phenomena by the energy of the exciting illumination which is necessary to generate carriers. This energy is called optical threshold energy. It is well known that illumination energies smaller than the band gap of $Al_xGa_{1-x}As$ are sufficient to cause PPC in this material. During illumination electrons are photoexcited from the deep donor into the conduction band. In selectively doped heterostructures, however, energies higher than the band gap of GaAs also give rise to PPC,[26] because a band-to-band electron-hole generation and a subsequent spatial separation of electron-hole pairs occurs.

We have measured the resistance of a selectively doped heterostructure at different illumination wavelengths.

The results are shown in Fig. 11. The monochromator was tuned during 360 s from $\lambda=1700$ to $\lambda=1000$ nm using several illumination intensities. When the illumination wavelength is changed from 1300 to 1100 nm, a drastic decrease of the sample resistance occurs which is due to the photoionization of the deep donors in $n$-type $Al_xGa_{1-x}As$. The exact value of the resistance decrease depends on the illumination intensity. Within this uncertainty the optical ionization energy is determined to be $E_{do}=0.95$ to 1.10 eV. During measurements band-to-band excitation of electron-hole pairs in the GaAs layer is inhibited by using several optical filters with cutoff at 1000 nm. It is important to note that the observed optical ionization energy is well below the band-gap energy of both GaAs and $Al_xGa_{1-x}As$.

We now compare quantitatively the two PPC mechanisms of photoexcitation of the deep donor in the $Al_xGa_{1-x}As$ layer and electron-hole pair generation in the GaAs layer with subsequent charge separation. The heterostructure is illuminated by light of wavelengths from 1200 to 800 nm. The result of these experiments is shown in Fig. 12. The wavelength which corresponds to the GaAs band-gap energy at 4.2 K is indicated in the figure. The wavelength is tuned during 9 min. At a wavelength of 1200 nm a strong decrease of the sample resistance is observed which saturates after some minutes. However, only a small change of the resistance is observed when the illumination energy corresponds to the band-gap energy of GaAs. The contribution from the GaAs layer to the photoconductivity of the heterostructure is thus relatively small as compared to the deep Si-donor ionization in the $Al_xGa_{1-x}As$ layer for the specific sample of Fig. 12.

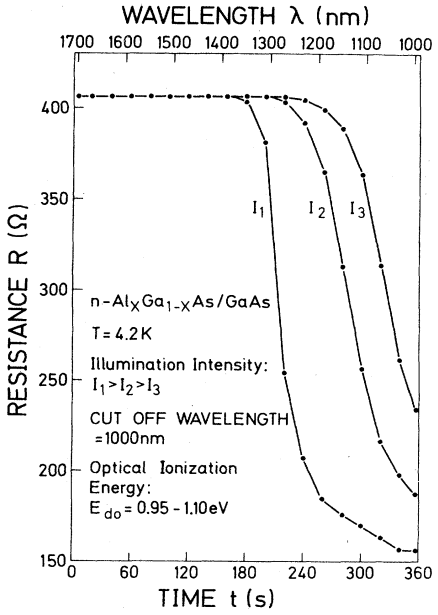


FIG. 11. Optical threshold wavelength of the deep-Si-donor ionization in the constituent $Al_xGa_{1-x}As$ layer of the heterostructure. The optical threshold energy depends weakly on the illumination intensity and is measured to be $E_{do}=0.95-1.10$ eV.

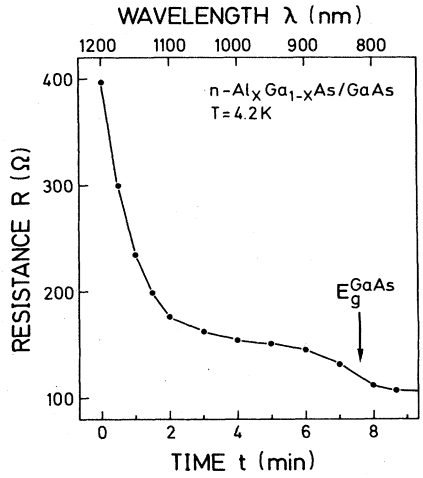


FIG. 12. Resistance of a selectively doped heterostructure versus illumination wavelength. The contribution to persistent photoconductivity of both the deep Si donor in $Al_xGa_{1-x}As$ and the band-to-band electron-hole generation in the GaAs are separated via the exciting illumination wavelength. The contribution of the latter process is comparatively small.

The relative contributions of the deep Si donor in the $Al_xGa_{1-x}As$ layer and the band-to-band excitation in the GaAs layer rely on the concentration of the deep Si donor in the $Al_xGa_{1-x}As$. This latter concentration, however, depends strongly on the alloy composition $x$.[24] Consequently, also, the relative contributions of the two photoconductive mechanisms depends on the alloy composition of the doped $Al_xGa_{1-x}As$. The alloy composition of the $Al_xGa_{1-x}As$ layer of the sample used in our measurement is $x\simeq 38\%$.

We have also prepared selectively $p$-type doped $Al_xGa_{1-x}As/GaAs$ heterostructures with the same alloy composition which exhibit very high hole mobilities especially at low temperatures. In $p$-type heterostructures no photoconductivity related to impurities is known, so that only a band-to-band electron-hole generation and a subsequent charge separation could cause PC. Photogenerated holes increase the concentration of the two-dimensional hole gas, and electrons drift to the substrate where they are trapped by deep acceptors (e.g., Cr or defect centers) in the semi-insulating substrate. Our experimental results of Hall-effect measurements on SD $p$-type heterostructures show that at 77 K the carrier concentration increases by less than 10% due to illumination. Störmer *et al.*[27] have detected no persistent photoconductivity at all in $p$-type SD heterostructures. These results confirm that band-to-band electron-hole generation and the following separation of the charge carriers plays only a minor role for persistent photoconductivity in SD heterostructures.

In addition to the optical threshold of the persistent photoconductivity we have also examined the optical threshold of the transient photoconductivity. The change of the resistance during the first 5 min as a function of the illumination wavelength is displayed in Fig. 13. The onset of the transient part of photoconductivity occurs at

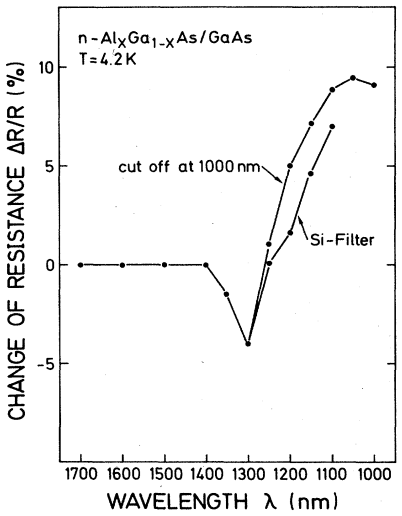


FIG. 13. Optical threshold wavelength of the transient photoconductivity (TPC) in a selectively doped heterostructure. The change of the resistance is determined from the sample resistance during illumination and 5 min after termination of the illumination.

about $\lambda = 1200$ nm. This threshold wavelength is the same as the deep donor ionization wavelength shown in Fig. 11. Therefore, both the transient and the persistent part of photoconductivity in heterostructures are caused by the deep Si donor of the $Al_xGa_{1-x}As$ layer. Transient photoconductivity is caused by deep Si donors localized in the $Al_xGa_{1-x}As$ close to the 2D EG. Electrons can easily tunnel to the impurities and recombine. Persistent photoconductivity is consequently predominantly caused by deep donors localized in the $Al_xGa_{1-x}As$ layer further away from the 2D EG. The larger distance reduces the tunneling probability significantly.

Transient photoconductivity is found to occur only in SD heterostructures at 4.2 K, but it is much less pronounced in bulk $n$-type $Al_xGa_{1-x}As$. We interpret this difference in terms of the kinetic energy of electrons at 4.2 K. Electrons in the conduction band of bulk material have the kinetic energy $\frac{3}{2}kT$. In contrast, electrons which occupy the subband of a triangular potential well with the subband energy $E_0$ have a kinetic energy $E_0$ due to the motion of electrons perpendicular to the potential well. At 4.2 K $E_0$ is about 200 times larger than the thermal energy $\frac{3}{2}kT$. Consequently the high-energy electrons in the subband of a quantum well are more likely to recombine after tunneling with the deep donor than the low-energy electrons of bulk $Al_xGa_{1-x}As$.

## V. CONCLUSION

We have in detail investigated and analyzed the electron-impurity tunneling occurring in selectivity doped $n$-type $Al_xGa_{1-x}As/GaAs$ heterostructures grown by molecular-beam epitaxy. For a quantitative evaluation the lowest subband energy of a triangular potential well at the $Al_xGa_{1-x}As$ interface is calculated by matching the electron—de Broglie wavelength to the potential well width. The result compares well with other calculations. In addition, the time-dependent carrier concentration, after termination of the exciting illumination, is calculated *analytically* in terms of a power series. We show that the decay of the carrier concentration is comparable to a logarithmic decay but it is definitely nonexponential. The nonexponential character of the carrier concentration versus time curve is experimentally confirmed. The time constant $\tau$ of the decay is *not* constant, but increases continuously with time. The time constant $\tau_0$ which applies to the initial decay, i.e., when the illumination is switched off, is determined at several temperatures by two independent methods. We have found that the time constant decreases significantly at enhanced temperatures. This decrease is due to the increasing capture cross section of the impurity level with temperature.

The plot of the carrier concentration versus logarithmic time is extrapolated to the dark carrier concentration to obtain an estimate of the total photoconductivity lifetime. The selectively doped heterostructure is expected to reach thermal equilibrium at $T \leqq 77$ K in $3 \times 10^4$ years after the illumination is turned off.

We performed wavelength-resolved optical excitation experiments to separate the two contributions to photoconductivity in heterostructures, namely the deep Si-donor excitation in the $Al_xGa_{1-x}As$ layer as well as the band-to-band electron-hole generation in the GaAs layer, and to determine their relative contributions quantitatively. The important result is that the band-to-band electron-hole generation in the GaAs gives only a small contribution to the observed photoconductivity. Finally, the optical threshold wavelength of the transient part of photoconductivity is measured to be $\lambda = 1200$ nm. This wavelength coincides with the deep-Si-donor optical ionization energy in the $Al_xGa_{1-x}As$ layer. This deep Si donor in $n$-type $Al_xGa_{1-x}As$ is therefore the origin for TPC. TPC is observed only in heterostructures owing to the much higher kinetic energy of electrons of the 2D EG at 4.2 K compared to the thermal energy of electrons in bulk material.

## ACKNOWLEDGMENTS

The authors would like to thank J. Knecht for expert help in sample preparation, K. Graf for essential assistance in computing procedures, and E. Rosencher (Centre National d'Etudes des Télécommunications, Meylan, France) for providing much helpful information. Thanks are also due to F. Stützler for a critical reading of the manuscript.

[1]H. L. Störmer, R. Dingle, A. C. Gossard, W. Wiegmann, and M. D. Sturge, Solid State Commun. **29**, 705 (1979).
[2]G. Abstreiter and K. Ploog, Phys. Rev. Lett. **42**, 1308 (1979).
[3]*Physics of Nonlinear Transport in Semiconductors,* edited by D. K. Ferry, J. R. Baker, and C. Jacoboni (Plenum, New York, 1980).
[4]Y. Suzuki, M. Seki, and H. Okamoto, in Proceedings of the 16th International Conference on Semiconductor Devices and Materials, Kobe, Japan, August 30—September 1 (1984) (unpublished).
[5]R. Dingle, H. L. Störmer, A. C. Gossard, and W. Wiegmann Appl. Phys. Lett. **33**, 665 (1978).
[6]E. F. Schubert and K. Ploog, Phys. Rev. B **29**, 4562 (1984).
[7]T. J. Drummond, W. Kopp, R. Fischer, H. Morkoc, R. E. Thorne, and A. Y. Cho, J. Appl. Phys. **53**, 1238 (1982).
[8]J. F. Rochette, P. Delescluse, M. Laviron, D. Delagebeaudeuf, J. Cherrier, and N. T. Linh, in *GaAs and Related Compounds,* edited by G. E. Stillman (IOP, London, 1982), p. 385.
[9]*Tunneling Phenomena in Solids,* edited by E. Burstein and S. Lundqvist (Plenum, New York, 1969).
[10]R. H. Fowler, and L. Nordheim, Proc. R. Soc. London, Ser. A **119**, 173 (1928).
[11]J. G. Simmons, J. Appl. Phys. **34**, 1793 (1963).
[12]L. L. Chang, L. Esaki, and R. Tsu, Appl. Phys. Lett. **24**, 593 (1974).
[13]K. Ploog and G. H. Döhler, Adv. Phys. **32**, 285 (1983).
[14]R. Dingle, in *Festkörperprobleme,* edited by H. J. Queisser (Vieweg, Braunschweig, 1975), p. 21.
[15]F. Stern, Phys. Rev. B **5**, 4891 (1972).
[16]T. Ando, J. Phys. Soc. Jpn. **51**, 3893 (1982).
[17]T. Ando, A. B. Fowler, and F. Stern, Rev. Mod. Phys. **54**, 437 (1982).
[18]D. Delagebeaudeuf and N. T. Linh, IEEE Trans. Electron Devices **ED-29**, 955 (1982).
[19]R. C. Miller, A. C. Gossard, D. A. Kleinmann, and O. Munteanu, Phys. Rev. B **29**, 3740 (1984).
[20]J. Curie, Ann. Chim. Phys. **17**, 385 (1889); **18**, 203 (1889); E. von Schweidler, Ann. Phys. **24**, 711 (1907). Recent work on the Curie—von Schweidler law was done by T. C. Guo and W. W. Guo, J. Phys. C **16**, 1955 (1983); A. K. Jonscher and R. M. Hill, *Dielectric Materials, Measurements and Applications* (IEE, London, 1979), Vol. 177, p. 164.
[21]H. J. Queisser, in *Proceedings of the 17th International Conference on the Physics of Semiconductors, San Francisco (1984),* edited by D. J. Chadi (Springer, New York, 1985).
[22]E. F. Schubert, K. Ploog, H. Dämbkes, and K. Heime Appl. Phys. A **33**, 63 (1984).
[23]H. Künzel, K. Ploog, K. Wünstel, and B. L. Zhou, J. Electron. Mater. **13**, 281 (1984).
[24]E. F. Schubert and K. Ploog, Phys. Rev. B **30**, 7021 (1984).
[25]B. L. Zhou, K. Ploog, E. Gmelin, X. Q. Zeng, and M. Schulz, Appl. Phys. A **28**, 223 (1982).
[26]A. Kastalsky and J. C. M. Hwang, Solid State Commun. **51**, 317 (1984).
[27]H. L. Störmer, A. C. Gossard, W. Wiegmann, R. Blondel, and K. Baldwin, Appl. Phys. Lett. **44**, 139 (1984).